

# HMT: Hierarchical Memory Transformer for Long Context Language Processing

Zifan He<sup>1</sup> Zongyue Qin<sup>1</sup> Neha Prakriya<sup>1</sup> Yizhou Sun<sup>1</sup> Jason Cong<sup>1</sup>

## Abstract

Transformer-based large language models (LLM) have been widely used in language processing applications. However, most of them restrict the context window that permits the model to attend to every token in the inputs. Previous works in recurrent models can memorize past tokens to enable unlimited context and maintain effectiveness. However, they have “flat” memory architectures, which have limitations in selecting and filtering information. Since humans are good at learning and self-adjustment, we speculate that imitating brain memory hierarchy is beneficial for model memorization. We propose the Hierarchical Memory Transformer (HMT), a novel framework that enables and improves models’ long-context processing ability by imitating human memorization behavior. Leveraging memory-augmented segment-level recurrence, we organize the memory hierarchy by preserving tokens from early input token segments, passing memory embeddings along the sequence, and recalling relevant information from history. Evaluating general language modeling (Wikitext-103, PG-19) and question-answering tasks (PubMedQA), we show that HMT steadily improves the long-context processing ability of context-constrained and long-context models. With an additional 0.5% ~ 2% of parameters, HMT can easily plug in and augment future LLMs to handle long context effectively. Our code is open-sourced on Github: <https://github.com/OswaldHe/HMT-pytorch>.

## 1. Introduction

Transformer (Vaswani et al., 2017) has demonstrated its strength in contextual learning and is utilized in various applications in language processing (Dong et al., 2019) and

<sup>1</sup>Department of Computer Science, University of California, Los Angeles, USA. Correspondence to: Zifan He <zifanhe1202@g.ucla.edu>.

computer vision (Dosovitskiy et al., 2020). For a decoder-only transformer model, each transformer block contains a self-attention and a feedforward network module. An optimized self-attention layer has a quadratic computational and linear space complexity (Dao et al., 2022) regarding the sequence length since it computes interactions between each token and all previous tokens in the sequence. To maintain the inference speed and satisfy memory requirements, most transformer models enforce maximum sequence length. For example, the Llama 2 model is designed to process 4096 tokens at maximum (Touvron et al., 2023). However, real-world applications involving long documents, such as book summarization (Rae et al., 2019) and lifelong question-answering tasks (Sun et al., 2019; Dai et al., 2022), can have an extensive number or even infinite stream of inputs.

Existing research attempts to build long-range transformers using sparse attention (Beltagy et al., 2020; Zhang et al., 2021; Kitaev et al., 2020), retrieval-augmented models (Bertsch et al., 2023; Wu et al., 2022), and recurrent sequence models (Peng et al., 2023; Gu & Dao, 2023; Rae et al., 2019). However, these models have at least one of two issues: (1) difficult to train or adapt to other models due to a change in the core model architecture and (2) low effectiveness for long-range inputs with frequent context switching. In this work, we propose the Hierarchical Memory Transformer (HMT), a novel framework to enable and enhance the long-context language processing ability of *any model*. HMT transforms any pretrained model into a memory-augmented segment-level recurrent model that imitates the brain’s memory hierarchy and human memorization behavior. It has the unique features as follows:

**Hierarchical Memorization:** HMT mimics the memory hierarchy of the brain (Burgin, 2011) employing both learned memory tokens and past input tokens. HMT stratifies memory into sensory, short-term, and long-term, with interactions between each other.

**Memory Recall Mechanism:** HMT imitates memory recall by storing encoded memory embeddings generated from previous iterations and searching based on the relevance to current token segments. It also handles inputs switching between multiple relevant topics.

One key advantage of using HMT over other memory-augment models is that HMT is a **model-independent plug-and-play** framework: future decoder-only models can directly use HMT without extra implementations. With joint training and fine-tuning of newly introduced parameters and original parameters of the backbone model, evaluation exhibits HMT’s advantage when applied to various models. Our impacts include:

- **HMT applies to any models with a short and limited context window to enable learning infinitely long context with enhanced effectiveness<sup>1</sup>, especially with context switching.** We demonstrate that with HMT, OPT and OpenLlamaV2 can be 25.5% and 17.6% more effective in perplexity (PPL) on Wikitext-103 with multiple samples concatenated, and 11.4% and 9.48% on PG-19, a book dataset. We also evaluated HMT with Llama 2 7B regarding the PubMedQA dataset with multiple contexts. It was 9.81% more effective in long-answer contextual reasoning with a 1.0% higher short-answer prediction accuracy.
- With a similar size state-of-the-art backbone model, **HMT outperforms various models designed for long context processing.** Moreover, **HMT can further increase the effectiveness of these long-context models.** For recurrent sequence models such as RWKV, HMT with OpenLlamaV2 is 44.0% and 14.9% more effective on Wikitext-103 and PG-19 respectively. Applying HMT to RWKV can further enhance effectiveness by 16.5% on Wikitext-103 and 9.96% on PG-19.
- **HMT is more effective than Recurrent Memory Transformer (RMT),** which is the previous state-of-the-art framework for augmenting models with a long context processing ability. HMT outperforms RMT by 13% for the Wikitext-103 dataset and 5.42% for the PG-19 dataset in PPL. HMT is also 8.98% more effective than RMT for long-answer contextual reasoning and 1.8% more accurate in short-answer prediction over QA tasks, indicating the advantage in long-context question-answering tasks.

## 2. Related Works and Problem Formulation

We will first discuss the existing efforts on long-range transformers and recurrent sequence models for infinitely long context language processing. Then, we highlight a problem that is crucial in real-world applications.

### 2.1. Long-range Transformer

Since one of the bottlenecks of transformers is the quadratic computational complexity of self-attention, a natural approach is sparsifying attention computation. A naive sparse

<sup>1</sup>In this paper, *effectiveness* means how well the language model generates meaningful texts. We measure it by perplexity

attention pattern is the sliding window attention (Kovaleva et al., 2019), where each token attends to neighbors within a local window. However, this neglects long-range interaction between words. Existing works such as Longformer (Beltagy et al., 2020) and Poolingformer (Zhang et al., 2021) extend the sliding window attention by adding global attending tokens and applying pooling to increase the receptive field area. Unlimiformer (Bertsch et al., 2023) adopts the retrieval-augmented generative model by searching the top K most important tokens for the incoming sequence and applying attention in the decoders to just those tokens, which prunes computations with minor loss. Nevertheless, the contribution of less relevant tokens may accumulate over time and impact the overall sequence generation. Although these methods extend the attainable context length, they cannot prevent increasing memory consumption as the input length increases. Alternatively, compressing past tokens using a recurrent sequence model can potentially reduce memory consumption by compressing information into a fixed-size embedding.

### 2.2. Recurrent Sequence Model

Recurrent Neural Networks (RNN) have been extensively explored in sequence processing research, including Long Short-term Memory (Hochreiter & Schmidhuber, 1997) and Gated Recurrent Unit (Chung et al., 2014). They reveal strong performance in memorizing past information and are hardware-friendly for implementing customized accelerators (Chang et al., 2015). However, RNNs have limited advantages compared with self-attention in learning contextual relationships between words in language processing (Bahdanau et al., 2014). One approach to alleviate this issue is the coarse-grain recurrence, in which the model splits inputs into segments, performs attention inside each segment, and propagates states between segments. The Compressive Transformer (Rae et al., 2019) further stores and compresses previous states to enhance memorization. The Recurrent Memory Transformer (RMT) (Bulatov et al., 2022) utilizes a memory token to summarize and propagate segment information without modifying the transformer block architecture. Theoretically, they can process unlimited long sequences, but previous information will be diluted after multiple summarizations and generation quality can drop when less relevant information occupies the memory. Nevertheless, it provides an important building block for HMT.

Another approach augments RNN that involves interactions between the current inputs and the previous states to learn contextual relationships in a similar way as self-attention and accelerate the computation with linear convolution. One of the representatives, RWKV (Peng et al., 2023), is an RNN model inspired by the attention-free transformer (AFT) (Zhai et al., 2021). It includes a time-mixing module to

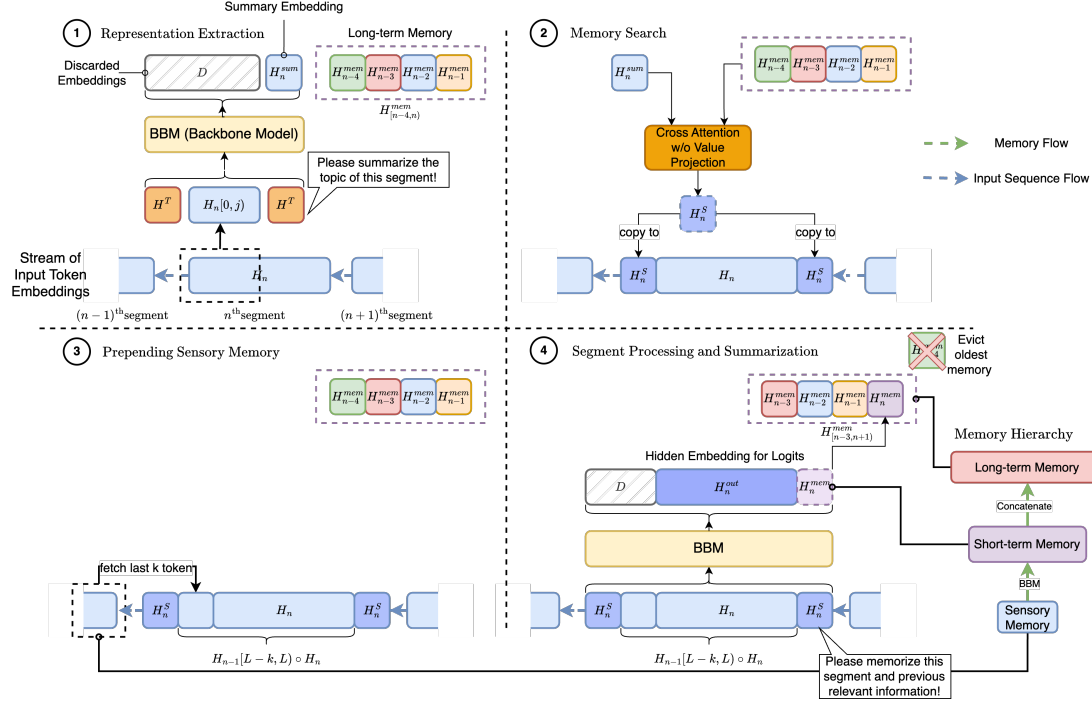


Figure 1. Overall workflow of HMT. (1) For a given segment of tokens, HMT will first perform **representation extraction** utilizing the segment summarization prompt embedding ( $H^T$ ) to summarize part of the segment. (2) The generated segment summary embedding ( $H_n^{sum}$ ) is used with the cached memory embeddings for **memory search** with cross attention. The output is a memorization prompt embedding ( $H_n^S$ ) which contains information relevant to the current segment and can guide the summarization in Step 4. (3) The memorization prompt embedding and the last  $k$  embeddings from the previous segment will augment the segment. (4) The backbone model (BBM) will process the augmented segment and generate hidden embeddings for logits ( $H_n^{out}$ ) and the memory embedding of the  $n^{th}$  segment ( $H_n^{mem}$ ), which will be pushed into the cache containing previous memory embeddings.

Table 1. Notation used to illustrate HMT’s architecture in Section 3 and Figure 1.

NOTATION	MEANING
$H_n$	HIDDEN EMBEDDINGS OF THE $n^{th}$ SEGMENT
$L$	SEGMENT LENGTH
$H_n[L-k, L]$	LAST $k$ EMBEDDINGS OF $H_n$
$H_n[0, j)$	FIRST $j$ EMBEDDINGS OF $H_n$
BBM(*)	BACKBONE MODEL
$H_n^S$	MEMORIZATION PROMPT EMBEDDING
$H_n^{out}$	HIDDEN EMBEDDING FOR LOGITS GENERATION
$H_n^{mem}$	MEMORY EMBEDDING OF THE $n^{th}$ SEGMENT
$D$	DISCARDED EMBEDDINGS
$N$	NUMBER OF CACHED MEMORY EMBEDDINGS
$H_{[n-N+1, n]}^{mem}$	CACHED MEMORY EMBEDDINGS
$H^T$	SEGMENT SUMMARIZATION PROMPT EMBEDDING
$H_n^{sum}$	SUMMARY EMBEDDING OF THE $n^{th}$ SEGMENT

learn from previous states and a channel-mixing module to learn from the previous output. Mamba (Gu & Dao, 2023) is a state-space model that employs gated convolution to accelerate the inference of recurrence. These models are energy and memory-efficient with fast training speed but

have limitations on recalling information from a very large document.

### 2.3. Problem Formulation: Adaptive Long-context Processing

We aim to develop a model that processes long-context information adaptively with the following properties:

*Continuous learning:* The model can process an infinite stream of data and gradually improve the performance when processing similar data.

*Context Adaptability:* Based on the context/topic of the input stream, the model can adaptively select past relevant information to enhance effectiveness, since irrelevant context can distract the model (Shi et al., 2023).

In real-world applications, restrained by memory bandwidth and capacity, as well as data generation speed, long documents cannot be read as a whole by the computing hardware (Agerri et al., 2015). Furthermore, users who are constantly interacting with the language model can refer to the previous topic or switch to another topic that has high relevance to past information provided. To be effective, most recur-

rent models need to encode all previous inputs in the states, which can contain irrelevant information that will degrade the model’s effectiveness.

### 3. HMT Method

Table 1 describes all notations we use to illustrate the HMT architecture in this section.

#### 3.1. Overall Workflow

HMT processes input in units of segments of  $L$  tokens. For every segment, HMT walks through 4 steps as shown in Figure 1:

- 1) *Representation extraction*, which encodes partial segment as a single embedding.
- 2) *Memory search*, which utilizes the generated embedding as a query to find relevant information in the history.
- 3) *Prepending sensory memory*, which augments the segment to capture tokens in the previous segment and relevant history.
- 4) *Segment processing and summarization*, which processes the augmented segment to get hidden embeddings for generating logits and a memory embedding that summarizes the augmented segment.

The first two steps are the *memory recall mechanism* discussed in Section 3.2. Steps 3 and 4 are explained in Section 3.3 along with the concept of hierarchical memorization.

#### 3.2. Memory Recall Mechanism

To handle context switching and prevent the intervention of irrelevant context, HMT performs memory recall to extract related information from past knowledge. The memory recall mechanism involves three steps: representation extraction, memory search, and memory augmentation.

**Representation Extraction:** Depicted in Step 1 of Figure 1, HMT selects the first  $j$  embeddings from the hidden embeddings of the  $n^{th}$  segment,  $H_n$ , to extract the topic of the segment. The embeddings are augmented with the **segment summarization prompt embedding**  $H^T$ .  $H^T$  is a learnable parameter and is identical for every segment, deployed to prompt the backbone model (BBM) to summarize the segment from the first  $H^T$  to the second occurrence of  $H^T$ . Instead of extracting from the token embedding of BBM, we use a learnable embedding to allow a larger prompt embedding space for summarization. The backbone model will then process the augmented embeddings and generate a new embedding at the end of the output as the representation of

the segment:

$$D \circ H_n^{sum} = \text{BBM}([H^T \circ H_n[0, j) \circ H^T])$$

where  $D$  is the embedding that will be discarded,  $H_n^{sum}$  is the summary embedding of the  $n^{th}$  segment only, and  $\text{BBM}(*)$  represents the backbone model. It will be used for memory search. “ $\circ$ ” is the concatenation operator.

**Memory Search:** Presented in Step 2 of Figure 1,  $H_n^{sum}$  is utilized as a query to find relevant memory embeddings generated from Step 4 when processing previous segments. We store the last  $N$  embeddings ( $H_{[n-N+1,n]}^{mem}$ ) and then computes:

$$Q = H_n^{sum} W_q, K = H_{[n-N+1,n]}^{mem} W_k$$

$$H_n^S = \text{softmax}\left(\frac{QK^T}{\sqrt{d_h}}\right) H_{[n-N+1,n]}^{mem}$$

where  $d_h$  is the hidden dimension of the cross attention. The computation is similar to cross-attention without value and output projection.  $\text{Softmax}\left(\frac{QK^T}{\sqrt{d_h}}\right)$  calculates the normalized similarity score, and applying it directly to  $H_{[n-N+1,n]}^{mem}$  can ensure similar distributions of output value and old memory tokens. We expect that the projection  $W_q$  and  $W_k$  can be trained such that summarizations containing similar contexts have high attention scores after projections. In practice, it performs better than having the value and output projections.

The output of a memory search is a **memorization prompt embedding**  $H_n^S$  containing information relevant to the  $n^{th}$  segment. It will be applied to augment the  $n^{th}$  segment.

Notice that HMT’s memory is accumulative: the  $n^{th}$  memory embedding contains information of all previous  $n - 1$  segments, with a higher loss of information for older segments. Recalling memory aims at strengthening the relevant memory by rolling back to relevant topics.

The overhead of the memory recall mechanism can be hidden if implemented on configurable hardware, as explained in Appendix F.

#### 3.3. Hierarchical Memorization

Human memory can be categorized into three strata: sensory memory, short-term memory, and long-term memory (Burgin, 2011). Sensory memory refers to very short-term memory generated from sensory information, such as vision and hearing. Short-term and long-term memory are long-lasting memories, differentiated by how long they persist in the brain. HMT is inspired by this memory hierarchy.

**Sensory Memory:** Sensory memory for the  $n^{th}$  segment refers to the last  $k$  token embeddings of  $H_{n-1}, H_{n-1}[L -$

$k, L$ ). When inferencing the  $n^{th}$  segment, HMT will augment the corresponding token embeddings  $H_n$  by prepending it with  $H_n[L-k, L]$ , shown in Step 3 of Figure 1.

**Short-term Memory:** HMT will encode the segment into an embedding that serves as a “summarization” of the segment. First, HMT will append and prepend memorization prompt embedding  $H_n^S$  to the augmented segment, guiding the backbone model to encode the segment and relevant information into a summarization embedding. As depicted in Step 4 of Figure 1, we train HMT such that

$$\text{BBM}(H_n^S \circ H_{n-1}[L-k, L] \circ H_n \circ H_n^S) = D \circ H_n^{\text{out}} \circ H_n^{\text{mem}}$$

where  $H_n^{\text{mem}}$  is the memory embedding of the  $n^{th}$  segment.  $H_n^{\text{out}}$  is a collection of  $L$  hidden embeddings that will be used to generate logits.

**Long-term Memory:** Each generated memory embedding will be cached as the long-term memory. Based on the memory constraint of the hardware, HMT stores the most recent  $N$  memory embeddings. We denote these cached embeddings as  $H_{[n-N-1, n-1]}^{\text{mem}}$ . The cached embeddings will be utilized as the input of *memory recall mechanism* to generate the memorization token embedding  $H_n^S$  for each segment as illustrated in the previous section.

Note that the computation of short-term memory has some similarity to RMT (Bulatov et al., 2022), but HMT will employ the memorization prompt embeddings generated in the memory recall to augment the segments.

## 4. Training and Fine-tuning HMT

Since HMT introduces parameters for memory recall, we need to train new parameters and fine-tune the parameters of the backbone model cooperatively. Training HMT involves multiple segments of tokens to learn how to encode input tokens and retrieve information properly. This section will demonstrate the efficiency of HMT in long-context training and the multi-stage strategy to increase the training speed.

### 4.1. Long-context Training

Both HMT and RMT are trained using backward propagation through time (BPTT) (Mozer, 2013), a technique utilized to train the RNN model by unrolling recurrent forward passes of the model to optimize long-sequence learning. One issue with RMT training with BPTT is the gradient explosion and vanishing problem. With a higher BPTT unroll depth, the effectiveness of RMT will first increase and then decrease, with a slow reduction or even an increase in training loss. Figure 2 depicts the effectiveness of RMT with the OPT 2.7B backbone model assessed over the Wikitext-103 dataset with various BPTT unroll depths. For both 2k and 10k token inputs, we observe a rising PPL when unrolling more than 5 segments during training.

On the contrary, HMT will not suffer from gradient vanishing or explosion as BPTT unroll depth increases due to the memory recall mechanism. Table 2 reveals that HMT can improve its effectiveness continuously as the BPTT unroll depth increases during training. Therefore, HMT will be more effective when the BPTT unroll depth increases. A detailed gradient stability analysis is presented in Appendix G. Furthermore, we applied several techniques to optimize the GPU memory consumption to increase the maximum trainable BPTT unroll depth compared with RMT, described in Appendix H.

Table 2. Relationship between the BPTT unroll depth and the test PPL of Wikitext-103 for OPT 2.7B with HMT. The experiment is evaluated on samples with 10k tokens. HMT preserved 32 tokens from the previous segment as the sensory memory and saved 300 memory embeddings for the memory recall. The segment size is 256 tokens.

BPTT UNROLL DEPTH	TEST PPL (WIKITEXT)
2	9.36
5	9.15
15	8.20

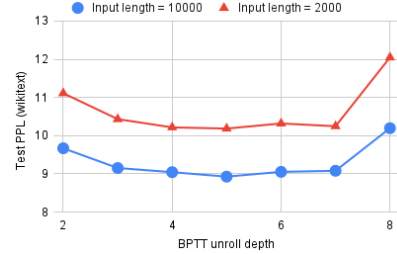


Figure 2. Effectiveness of training RMT with BPTT with different unroll depths for 2000 tokens and 10000 tokens input from the Wikitext-103 dataset. The backbone model is OPT 2.7B, with 256 tokens per segment during inference.

### 4.2. Multi-stage Training

Training HMT involves two stages. In the first stage, The model is trained without the memory recall mechanism employing BPTT with 2 segments unrolled. BPTT saves the model checkpoint locally. Then, the memory recall mechanism loads and extends the train model in the second stage. At this point, BPTT trains the modified model by unrolling the maximum number of segments that the GPUs can handle to maximize the effectiveness, which is 15 in our experiment. Since the architecture of HMT is complex, breaking up training into two stages is beneficial for local optimization and improves long context inference performance compared with single-stage training. Figure 3 exhibits the performance difference between the multi-stage and single-stage training of OPT 2.7B model with HMT

for long-context inputs. Since Stage 1 involves a shorter training sequence length and a simpler recurrent architecture than Stage 2, training with Stage 1 is faster per iteration (1.15 s/iteration) than Stage 2 (3.36 s/iteration). Within the same number of training steps, multi-stage training obtains better effectiveness and lower total training time than single-stage training.

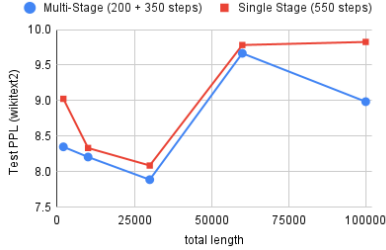


Figure 3. Training HMT + OPT 2.7B with the memory recall mechanism in two steps results in a better performance than using the mechanism to train HMT directly: first train the model without the memory recall, then load the checkpoint and train with the memory recall mechanism. Total training time is 902 s for multi-stage training and 1680 s for single-stage training on 4 AMD MI210 GPUs.

## 5. Experiment

We evaluate HMT and RMT with the same backbone models. Both HMT and RMT are benchmarked with a variety of backbone models including OPT 350M, OPT 2.7B (Zhang et al., 2022), OpenLlamaV2 (Geng & Liu, 2023) 3B, RWKV 3B (Peng et al., 2023), and Llama 2 7B (Touvron et al., 2023) models as the backbones. Moreover, we test several models with a long maximum context (Mamba 370M (Gu & Dao, 2023), Yi-6B-200K (Young et al., 2024), and Mistral 7B (Jiang et al., 2023)) to demonstrate the benefit HMT has on effectiveness and memory consumption. For general language modeling tasks, we select OPT 350M, OPT 2.7B, and OpenLlamaV2 3B as the representative of context-constrained models (models with a short maximum context window) and RWKV 3B and Mamba 370M for recurrent models. We evaluate the recurrent backbone model since we believe that HMT can be beneficial to these models that can already process infinitely long inputs. For the question-answering tasks, we employ Llama 2 7B as the backbone model. The largest model that our GPUs can handle has 7B parameters, but HMT produces consistently better performances over all these models to show that it can potentially be applied to larger models for an effectiveness boost. All models are trained and tested on 4 AMD MI210 GPUs. The baselines are evaluated using the sliding window attention for context-constrained models to control the memory consumption for a fair comparison. Due to the limited VRAM of GPUs, we shrink the segment length

for the larger backbone model. Also, increasing memory token size does not improve the effectiveness as Bulatov et al. suggested. Thus, both RMT and HMT apply memory tokens with a length of 1. For RMT, we utilize the maximum BPTT unroll depth with the best effectiveness that the GPUs can handle. HMT is trained with the multi-stage training technique illustrated in Section 4.2. The first stage (S1) is trained with 2 segments, and the second stage (S2) is trained with the maximum BPTT unroll depth that the GPUs can manage. We select the learning rate for HMT, RMT, and the baseline to optimize the effectiveness. Furthermore, HMT preserves 32 tokens from the previous segment as the sensory memory. All models are trained with 700 steps in total, which is sufficient to converge the training loss. Table 3 recaps the training configurations of different models in our experiments.

For general language tasks, models are tested for next token generation tasks with Wikitext-103 (Merity et al., 2016) and PG-19 (Rae et al., 2019) datasets. Wikitext-103 contains general knowledge from Wikipedia where each term definition has 2 - 3k words. Processing inputs with multiple definitions can simulate context switches. PG-19 is a benchmark that includes a set of books published before 1919 from the Project Gutenberg library, with an average length of 69k tokens. Samples will be concatenated or split into chunks with specified input lengths to investigate the relationships between input length and the effectiveness of the model. For question-answering tasks, we chose PubMedQA (Jin et al., 2019), which is a biomedical question-answering dataset with corresponding contexts. We artifact the long-context dataset as the following: (1) select  $M$  question-context-answer tuples from the dataset. Let this set of tuples be  $\{(C_0, Q_0, A_0), (C_1, Q_1, A_1), \dots, (C_T, Q_T, A_T)\}$ , where  $C_n$  are contexts,  $Q_n$  are questions,  $A_n$  are answers for  $0 \geq n \geq M$ . Answers can be either long answers with detailed reasoning or short answers (either “yes”, “no”, or “maybe”). (2) Concatenate all the contexts from each tuple to form a long context and append the questions and answers for each tuple. This will create  $M$  sequences:  $C_0C_1\dots C_TQ_0A_0, C_0C_1\dots C_TQ_1A_1, \dots, C_0C_1\dots C_TQ_TA_T$ . By controlling the value of  $M$ , we can determine the fraction of useful information in the context for each question and better understand the filtering and selection ability of HMT and the baseline model.

## 6. Results and Key Observations

### 6.1. Impacts on Context-constrained Models

By applying an additional  $0.5\% \sim 2\%$  of parameters, HMT can augment any context-constrained models to process long-context inputs. We demonstrate this feature with general language modeling tasks and question-answering tasks.

Table 3. Training configurations for the backbone models (OPT 350M, Mamba 370M, OPT 2.7B, RWKV 3B, OpenLlamaV2 3B, Llama 2 7B, YI-6B-200K, and Mistral 7B) and the modified model after applying RMT and HMT. S1 and S2 indicate the first stage and the second stage of multi-stage training for HMT. 4 AMD MI210 GPUs cannot train larger models. The given learning rate is the starting learning rate, and will decay by factor of 0.7 for every 100 steps. The batch size is 2.

MODEL	INPUT LENGTH	SEGMENT LENGTH	LEARNING RATE	TRAINING STEPS
OPT 350M	2048	1024	1E-5	700
+RMT	2048	1024	1E-5	700
+HMT (S1)	2048	1024	1E-5	200
+HMT (S2)	15360	1024	1E-5	500
OPT 2.7B / OPENLLAMA V2 3B	2048	256	1E-5	700
+RMT	1280	256	1E-5	700
+HMT (S1)	512	256	1E-5	200
+HMT (S2)	3840	256	1E-5	500
RWKV 3B	1280	256	1E-5	700
+RMT	1280	256	1E-4	700
+HMT (S1)	512	256	1E-5	200
+HMT (S2)	1280	256	1E-5	500
LLAMA 2 7B	2048	256	1E-4	700
+RMT	1280	256	1E-4	700
+HMT (S1)	512	256	1E-4	200
+HMT (S2)	2048	256	1E-4	500
MAMBA 370M	1536	256	1E-4	700
+HMT (S1)	512	256	1E-4	200
+HMT (S2)	1536	256	1E-4	500
YI-6B-200K / MISTRAL 7B	2048	-	2E-4	700
+HMT (S1)	1024	512	2E-4	200
+HMT (S2)	1536	512	2E-4	500

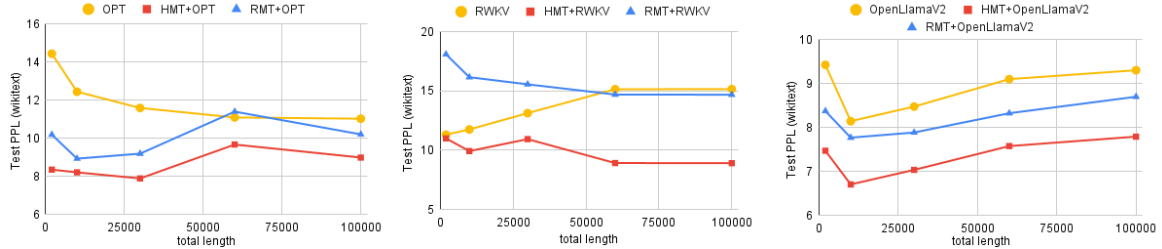


Figure 4. Effectiveness of HMT, RMT, and three baseline models (OPT 2.7B, RWKV 3B, OpenLlamaV2 3B) with the Wikitext-103 dataset. HMT outperforms RMT by 13.0% for OPT and 10.8% for OpenLlamaV2. For RWKV, HMT can even boost the effectiveness by 16.5%, while RMT worsens the effectiveness.

**HMT significantly improves the backbone models in general language modeling tasks when processing long inputs.** Figure 4 and 5 compare the effectiveness of OPT 2.7B and OpenLlamaV2 3B models with and without HMT on the Wikitext-103 and PG-19 datasets. Over input spanning from 2k ~ 100k tokens, HMT improves effectiveness by 25.5% for OPT and 17.6% for OpenLlamaV2 over the Wikitext-103 dataset. Moreover, for the PG-19 dataset, HMT enhances the effectiveness by 11.4% for OPT and 9.48% for OpenLlamaV2. In sum, HMT offers consistent benefits for context-constrained models.

**HMT enhances long-answer contextual reasoning and short-answer prediction ability in question-answering tasks.** One of the use cases of HMT is handling question-answering tasks that involve multiple contexts. Thus, we select the PubMedQA dataset and derive a long context QA benchmark to evaluate the effectiveness of HMT. We assess

HMT with Llama 2 7B as the backbone model, shown in Figure 6 and 7. Two metrics are employed: for long answers, we compute the PPL to evaluate the contextual reasoning of HMT; for short answers, we measure the response accuracy. For samples with  $M$  from 2 to 10, HMT increases the effectiveness in PPL by 9.48% for long answers. For short answer tasks, HMT is 1.0% more accurate than the backbone model. In sum, HMT boosts both the correctness and reasoning ability of context-constrained models in long-context QA tasks.

## 6.2. Comparison to Long Context Models

Combined with context-constrained models, HMT can be more effective than long-context models. For example, HMT with OpenLlamaV2 3B is 44.0% and 14.9% more effective on Wikitext-103 and PG-19 respectively. Moreover, applying HMT to long-context models can further



Figure 5. Effectiveness of HMT, RMT, and three baseline models (OPT 2.7B, RWKV 3B, OpenLlamaV2 3B), evaluated over the PG-19 dataset. HMT outperforms RMT by 3.98% for OPT and 6.85% for OpenLlamaV2. For RWKV, HMT can boost the effectiveness by 9.96%.

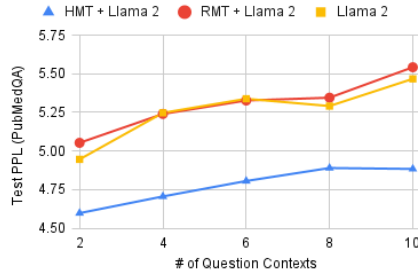


Figure 6. Effectiveness of RMT and HMT applied on Llama-2 7B, evaluated over PubMedQA dataset with modification for long context processing. The answer in each sample is the long answer. HMT is 8.98% more effective than RMT in PPL.

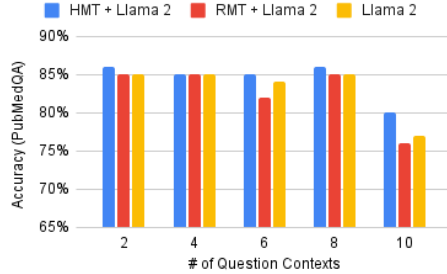


Figure 7. Response accuracy of RMT and HMT applied on Llama-2 7B, evaluated over PubMedQA dataset with modification for long context processing. The answer in each sample is the short answer. HMT is 1.8% more accurate than RMT on average.

improve their effectiveness. HMT can enhance the effectiveness of RWKV by 16.5% on Wikitext-103 and 9.96% on PG-19 as shown in Figure 4 and 5. Beyond recurrent models, HMT also has better effectiveness with reduced memory consumption, indicating the usefulness of memory augmentation. For example, the AMD MI210 GPU cannot handle inferencing 30k token inputs with the Yi-6B-200K model due to memory constraints. Applying a sliding window strategy with a 5.2K-token window (Yi-6B-SW-5.2K), the model consumes 44.8 GB VRAM. On the contrary, HMT + Yi-6B-200K requires only 33.9 GB VRAM to process

30k tokens with a small segment length (512 tokens), with 2% effectiveness improvement. Table 4 presents the effectiveness of long-range models on Wikitext-103 compared with several HMT-augmented models, including Mamba and Mistral models.

Table 4. Effectiveness of long context models and HMT with various backbone models. The input size is 30k tokens and the dataset is Wikitext-103. HMT not only outperforms long context models when applied to context-constrained models but also can further improve the effectiveness of these models.

MODEL	MAX CONTEXT	TEST PPL (WIKITEXT)
RWKV 3B	$\infty$	13.13
MAMBA 370M	$\infty$	87.08
YI-6B-200K	200K	OOM
YI-6B-SW-5.2K	200K	6.89
MISTRAL-7B	32K	5.47
HMT + OPT 350M	$\infty$	13.04
HMT + OPENLLAMA2 3B	$\infty$	7.04
HMT + RWKV 3B	$\infty$	10.94
HMT + MAMBA 370M	$\infty$	16.71
HMT + YI-6B-200K	$\infty$	6.75
HMT + MISTRAL-7B	$\infty$	5.12

Furthermore, compared with other memory-augmented models, HMT is not only easy to use but also more effective. The Memorizing transformer (Wu et al., 2022) is a memory-augmented long-context model. This model requires **training from scratch per downstream task** before inference, which is not user-friendly for general usage. We compared the Memorizing Transformer trained on the Wikitext-103 dataset with HMT + OPT 350M, which has a similar parameter count, shown in table 5. With only 700 training steps, HMT outperforms the Memorizing Transformer trained with 10k steps by 2x in perplexity, indicating that HMT is more efficient and effective to use.

Table 5. Effectiveness of Memorizing Transformer and HMT + OPT 350M models over Wikitext-103 dataset with 30k-token samples.

MODEL	TEST PPL (WIKITEXT)
MEMORIZING TRANSFORMER	31.51
HMT + OPT 350M	13.67

### 6.3. Comparison to RMT

Our assessment indicates that HMT is generally better at both language modeling and question-answering tasks than RMT. Figure 4 and 5 compare the effectiveness between HMT and RMT with the Wikitext-103 and PG-19 datasets. HMT improves the effectiveness by 13% for OPT and 10.8% for OpenLlamaV2 on the Wikitext-103 dataset compared with applying RMT. Moreover, in contrast to RMT on the PG-19 dataset, HMT performs 3.98% better for OPT and 6.85% better for OpenLlamaV2.

For recurrent sequence models, HMT can further increase the effectiveness of RWKV while RMT will degrade the performance for both datasets, as demonstrated in Figure 5. Since RWKV has already compressed past tokens and passed hidden states along the sequence, applying RMT to RWKV is simply re-weighting past information compressed in states periodically. This was originally done by the time-mixing module of RWKV. Therefore, the advantage of memory augmentation is limited. Due to the gradient vanishing issue mentioned in Appendix G, the model is harder to train with RMT, leading to inferior performance. However, we believe that the memory recall mechanism in HMT helps RWKV to select previous hidden states with the most relevance, boosting the effectiveness.

Evaluating with the PubMedQA dataset, HMT improves the effectiveness in PPL by 8.98% for long answers compared with RMT. For short answer tasks, HMT is 1.8% more accurate than RMT on average.

### 6.4. Ablation Study

We conduct ablation studies regarding the memory recall mechanism to demonstrate (1) memory recall is beneficial, (2) partial summarization of a segment in memory recall can speed up inference while maintaining similar effectiveness, and (3) caching more memory embedding can improve the effectiveness of HMT.

**Impact of memory recall mechanism.** Figure 8 displays the advantages of having a memory recall mechanism in HMT for long context input with context switching. For any tested input length, the effectiveness of HMT with memory recall outperforms that without memory recall. Furthermore, when the memory recall mechanism is deployed, the effectiveness improves for the OPT 350M backbone model or tends to improve for the OPT 2.7B backbone model as the input sequence length grows, demonstrating better scalability of HMT.

**Impact of summarizing partial segment in memory recall.** To overlap or reduce the inference time of the previous segment with the representation extraction of the next segment, it is necessary to prefetch only the first  $l$  tokens in the segment for summarization as described in Appendix

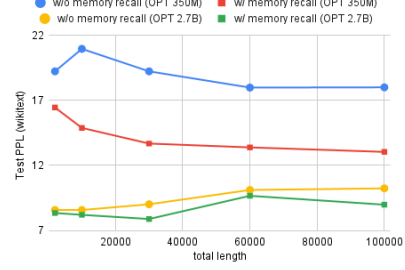


Figure 8. Effectiveness of HMT with and without memory recall mechanism for OPT 350M and 2.7B as the backbone models. The inputs are extracted from the Wikitext-103 dataset with up to 100k tokens.

**F.** In the experiment, we select half of the segment for representation extraction. We examine the model that extracts the whole segment and compare the effectiveness, depicted by Figure 9. The impact is negligible. We hypothesize that the start of a segment contains enough information about the overall topic for memory recall, which is intuitive as humans can capture the concepts by browsing keywords or segments instead of reading the whole paragraphs.

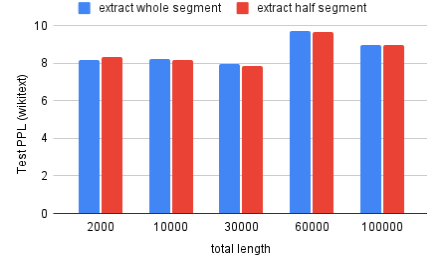


Figure 9. Effectiveness of HMT with OPT 2.7B when performing representation extraction on the whole segment for half of the segment. The impact is negligible, justifying that summarizing half of the segment is a valid method for inference acceleration.

**Impact of limited cached memory embeddings.** Due to memory constraints, we only cache the most recent 300 memory embeddings for memory recall. Figure 10 depicts the relationship between the number of cached memory embeddings and the effectiveness of HMT with Llama 2 7B over the Wikitext-103 dataset with 100k-token samples. We observed that increasing the window of cached memory benefits the effectiveness, but the improvement becomes marginal. We hypothesize that HMT is more likely to recall recent memory embeddings in the Wikitext-103 dataset. Figure 11 plots the frequency distribution of the distance between the current segment and the segment corresponding to the memory embedding with the highest softmax score in the memory recall mechanism. 6.5% of the segments retrieve memory tokens within 2 segments. This indicates the importance of local context. However, the long con-

text memory recall still exists. A possible explanation is that entries in Wikipedia may refer to other entries through hyperlinks and related context, and HMT discovers this long-context relationship and recalls the relevant information. For the PubMedQA dataset with multiple contexts concatenated, the long context recall also exists. We examine HMT with one sample containing 4 contexts illustrated in Figure 12. We inspect the highest softmax score of the memory recall cross attention when processing the segment that contains the questions and discover that it corresponds to the first context, which is the original context used for the question.

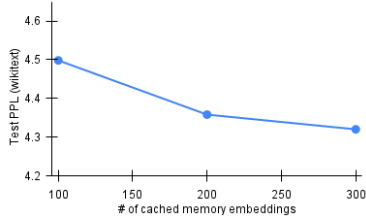


Figure 10. Relationship between number of cached memory embeddings and the effectiveness of HMT + Llama 2 7B. Each sample has 100k tokens from the Wikitext-103 dataset. As HMT stores more memory embeddings, the effectiveness is marginally better.

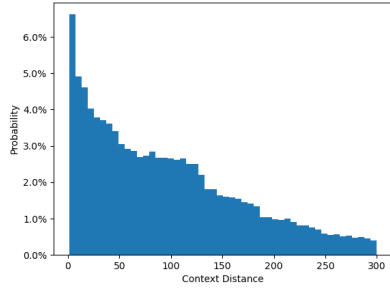


Figure 11. Histogram of context distance between the current segment and the segment corresponding to the memory embedding with the highest softmax score in the memory recall mechanism. The dataset evaluated is the Wikitext-103.

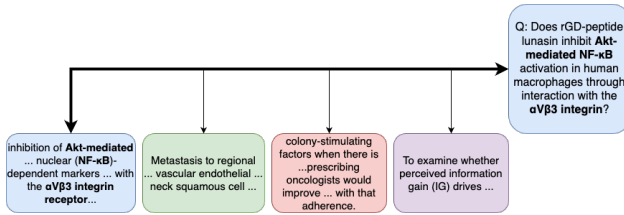


Figure 12. Example of HMT recalling the correct context in PubMedQA dataset with 4 contexts.

## 7. Conclusion and Ongoing Works

We present HMT, a framework to augment LLMs' long-range language processing ability with context switching. Inspired by the brain's memory hierarchy, HMT imitates human memorization behavior by deploying hierarchical memorization and the memory recall mechanism. Compared with other models that can process infinitely long inputs, HMT has a more stable and better effectiveness for input with context switching. HMT can be directly applied to any pretrained fixed-context models with higher BPTT unroll depth than RMT. Moreover, it can boost other long-range transformer models which are already effective in processing infinitely long input. Our model not only provides LLM accessibility to resource-constrained applications but also represents a step forward to lifelong language processing tasks.

Currently, HMT will remove the oldest memory token when the total number of memory tokens stored is above a context window  $N$ . Hence, the model cannot recall more than  $N$  segments. To recall any past segment, a possible solution is applying an extra hierarchy over the memory recall mechanism: we partition the memory tokens into segments and encode each segment into a tag vector. Memory recall requires encoding the current segment into a query tag and searching for the best memory token segment before computing the cross attention. Memory token segments can be stored throughout the machine (SSD, DRAM, and SRAM).

## 8. Ethical and Societal Impact

This work aims to advance the field of natural language processing. Specifically for HMT, it provides a foundation for building a lifelong AI assistant that can keep adapting to users' habits by continuously monitoring users' behavior, communicating with users, and memorizing experiences. Such an assistant offers convenience to people's daily lives, while also raising concerns about privacy leakage. Nevertheless, with further efforts to deploy it on edge devices without network connections, this issue can be resolved.

## Acknowledgement

This research is partially supported by the PRISM (000705769) center under the JUMP 2.0 program by DARPA/SRC and NSF SEED funding. It is also supported by CDSC industrial partners (<https://cdsc.ucla.edu/partners>) and the AMD HACC Program.

## References

Abdelkhalik, H., Arafa, Y., Santhi, N., and Badawy, A.-H. A. Demystifying the nvidia ampere architecture through microbenchmarking and instruction-level analysis. In 2022

IEEE High Performance Extreme Computing Conference (HPEC), pp. 1–8. IEEE, 2022.

Agerri, R., Artola, X., Beloki, Z., Rigau, G., and Soroa, A. Big data for natural language processing: A streaming approach. *Knowledge-Based Systems*, 79:36–42, 2015.

Bahdanau, D., Cho, K., and Bengio, Y. Neural machine translation by jointly learning to align and translate. *arXiv preprint arXiv:1409.0473*, 2014.

Beltagy, I., Peters, M. E., and Cohan, A. Longformer: The long-document transformer. *arXiv preprint arXiv:2004.05150*, 2020.

Bertsch, A., Alon, U., Neubig, G., and Gormley, M. R. Unlimiformer: Long-range transformers with unlimited length input. *arXiv preprint arXiv:2305.01625*, 2023.

Bulatov, A., Kuratov, Y., and Burtsev, M. Recurrent memory transformer. *Advances in Neural Information Processing Systems*, 35:11079–11091, 2022.

Burgin, M. Epistemic information in stratified m-spaces. *Information*, 2(4):697–726, 2011.

Chang, A. X. M. and Culurciello, E. Hardware accelerators for recurrent neural networks on fpga. In *2017 IEEE International symposium on circuits and systems (ISCAS)*, pp. 1–4. IEEE, 2017.

Chang, A. X. M., Martini, B., and Culurciello, E. Recurrent neural networks hardware implementation on fpga. *arXiv preprint arXiv:1511.05552*, 2015.

Chung, J., Gulcehre, C., Cho, K., and Bengio, Y. Empirical evaluation of gated recurrent neural networks on sequence modeling. *arXiv preprint arXiv:1412.3555*, 2014.

Dai, Y., Lang, H., Zheng, Y., Huang, F., Si, L., and Li, Y. Lifelong learning for question answering with hierarchical prompts. *arXiv preprint arXiv:2208.14602*, 2022.

Dai, Z., Yang, Z., Yang, Y., Carbonell, J., Le, Q. V., and Salakhutdinov, R. Transformer-xl: Attentive language models beyond a fixed-length context. *arXiv preprint arXiv:1901.02860*, 2019.

Dao, T., Fu, D., Ermon, S., Rudra, A., and Ré, C. Flashattention: Fast and memory-efficient exact attention with io-awareness. *Advances in Neural Information Processing Systems*, 35:16344–16359, 2022.

Dong, L., Yang, N., Wang, W., Wei, F., Liu, X., Wang, Y., Gao, J., Zhou, M., and Hon, H.-W. Unified language model pre-training for natural language understanding and generation. *Advances in neural information processing systems*, 32, 2019.

Dosovitskiy, A., Beyer, L., Kolesnikov, A., Weissenborn, D., Zhai, X., Unterthiner, T., Dehghani, M., Minderer, M., Heigold, G., Gelly, S., et al. An image is worth 16x16 words: Transformers for image recognition at scale. *arXiv preprint arXiv:2010.11929*, 2020.

Geng, X. and Liu, H. Openllama: An open reproduction of llama, May 2023. URL [https://github.com/openlm-research/open\\_llama](https://github.com/openlm-research/open_llama).

Gu, A. and Dao, T. Mamba: Linear-time sequence modeling with selective state spaces. *arXiv preprint arXiv:2312.00752*, 2023.

Guo, L., Chi, Y., Lau, J., Song, L., Tian, X., Khatti, M., Qiao, W., Wang, J., Ustun, E., Fang, Z., et al. Tapa: a scalable task-parallel dataflow programming framework for modern fpgas with co-optimization of hls and physical design. *ACM Transactions on Reconfigurable Technology and Systems*, 16(4):1–31, 2023.

Hochreiter, S. and Schmidhuber, J. Long short-term memory. *Neural computation*, 9(8):1735–1780, 1997.

Hu, E. J., Shen, Y., Wallis, P., Allen-Zhu, Z., Li, Y., Wang, S., Wang, L., and Chen, W. Lora: Low-rank adaptation of large language models. *arXiv preprint arXiv:2106.09685*, 2021.

Ioannou, L. and Fahmy, S. A. Streaming overlay architecture for lightweight lstm computation on fpga socs. *ACM Transactions on Reconfigurable Technology and Systems*, 16(1):1–26, 2022.

Jiang, A. Q., Sablayrolles, A., Mensch, A., Bamford, C., Chaplot, D. S., Casas, D. d. l., Bressand, F., Lengyel, G., Lample, G., Saulnier, L., et al. Mistral 7b. *arXiv preprint arXiv:2310.06825*, 2023.

Jin, Q., Dhingra, B., Liu, Z., Cohen, W. W., and Lu, X. Pubmedqa: A dataset for biomedical research question answering. *arXiv preprint arXiv:1909.06146*, 2019.

Khatti, M., Tian, X., Chi, Y., Guo, L., Cong, J., and Fang, Z. Pasta: Programming and automation support for scalable task-parallel hls programs on modern multi-die fpgas. In *2023 IEEE 31st Annual International Symposium on Field-Programmable Custom Computing Machines (FCCM)*, pp. 12–22. IEEE, 2023.

Khoda, E. E., Rankin, D., de Lima, R. T., Harris, P., Hauck, S., Hsu, S.-C., Kagan, M., Loncar, V., Paikara, C., Rao, R., et al. Ultra-low latency recurrent neural network inference on fpgas for physics applications with hls4ml. *Machine Learning: Science and Technology*, 4(2):025004, 2023.

Kitaev, N., Kaiser, Ł., and Levskaya, A. Reformer: The efficient transformer. *arXiv preprint arXiv:2001.04451*, 2020.

Kovaleva, O., Romanov, A., Rogers, A., and Rumshisky, A. Revealing the dark secrets of bert. *arXiv preprint arXiv:1908.08593*, 2019.

Li, H., Yu, D., Kumar, A., and Tu, Y.-C. Performance modeling in cuda streams—a means for high-throughput data processing. In *2014 IEEE international conference on big data (big data)*, pp. 301–310. IEEE, 2014.

Merity, S., Xiong, C., Bradbury, J., and Socher, R. Pointer sentinel mixture models. *arXiv preprint arXiv:1609.07843*, 2016.

Modarressi, A., Imani, A., Fayyaz, M., and Schütze, H. Retilm: Towards a general read-write memory for large language models. *arXiv preprint arXiv:2305.14322*, 2023.

Moro, G., Ragazzi, L., Valgimigli, L., Frisoni, G., Sartori, C., and Marfia, G. Efficient memory-enhanced transformer for long-document summarization in low-resource regimes. *Sensors*, 23(7):3542, 2023.

Mozer, M. C. A focused backpropagation algorithm for temporal pattern recognition. In *Backpropagation*, pp. 137–169. Psychology Press, 2013.

Pascanu, R., Mikolov, T., and Bengio, Y. On the difficulty of training recurrent neural networks. In *International conference on machine learning*, pp. 1310–1318. Pmlr, 2013.

Peng, B., Alcaide, E., Anthony, Q., Albalak, A., Arcadinho, S., Cao, H., Cheng, X., Chung, M., Grella, M., GV, K. K., et al. Rwkv: Reinventing rnns for the transformer era. *arXiv preprint arXiv:2305.13048*, 2023.

Rae, J. W., Potapenko, A., Jayakumar, S. M., and Lillicrap, T. P. Compressive transformers for long-range sequence modelling. *arXiv preprint arXiv:1911.05507*, 2019.

Rajbhandari, S., Rasley, J., Ruwase, O., and He, Y. Zero: Memory optimizations toward training trillion parameter models. In *SC20: International Conference for High Performance Computing, Networking, Storage and Analysis*, pp. 1–16. IEEE, 2020.

Rasley, J., Rajbhandari, S., Ruwase, O., and He, Y. Deep-speed: System optimizations enable training deep learning models with over 100 billion parameters. In *Proceedings of the 26th ACM SIGKDD International Conference on Knowledge Discovery & Data Mining*, pp. 3505–3506, 2020.

Shi, F., Chen, X., Misra, K., Scales, N., Dohan, D., Chi, E. H., Schärlí, N., and Zhou, D. Large language models can be easily distracted by irrelevant context. In *International Conference on Machine Learning*, pp. 31210–31227. PMLR, 2023.

Sun, F.-K., Ho, C.-H., and Lee, H.-Y. Lamol: Language modeling for lifelong language learning. *arXiv preprint arXiv:1909.03329*, 2019.

Touvron, H., Martin, L., Stone, K., Albert, P., Almahairi, A., Babaei, Y., Bashlykov, N., Batra, S., Bhargava, P., Bhosale, S., et al. Llama 2: Open foundation and fine-tuned chat models. *arXiv preprint arXiv:2307.09288*, 2023.

Vaswani, A., Shazeer, N., Parmar, N., Uszkoreit, J., Jones, L., Gomez, A. N., Kaiser, Ł., and Polosukhin, I. Attention is all you need. *Advances in neural information processing systems*, 30, 2017.

Wang, W., Dong, L., Cheng, H., Liu, X., Yan, X., Gao, J., and Wei, F. Augmenting language models with long-term memory. *Advances in Neural Information Processing Systems*, 36, 2024.

Wu, Q., Lan, Z., Qian, K., Gu, J., Geramifard, A., and Yu, Z. Memformer: A memory-augmented transformer for sequence modeling. *arXiv preprint arXiv:2010.06891*, 2020.

Wu, Y., Rabe, M. N., Hutchins, D., and Szegedy, C. Memorizing transformers. *arXiv preprint arXiv:2203.08913*, 2022.

Young, A., Chen, B., Li, C., Huang, C., Zhang, G., Zhang, G., Li, H., Zhu, J., Chen, J., Chang, J., et al. Yi: Open foundation models by 01. ai. *arXiv preprint arXiv:2403.04652*, 2024.

Zhai, S., Talbott, W., Srivastava, N., Huang, C., Goh, H., Zhang, R., and Susskind, J. An attention free transformer. *arXiv preprint arXiv:2105.14103*, 2021.

Zhang, H., Gong, Y., Shen, Y., Li, W., Lv, J., Duan, N., and Chen, W. Poolingformer: Long document modeling with pooling attention. In *International Conference on Machine Learning*, pp. 12437–12446. PMLR, 2021.

Zhang, S., Roller, S., Goyal, N., Artetxe, M., Chen, M., Chen, S., Dewan, C., Diab, M., Li, X., Lin, X. V., et al. Opt: Open pre-trained transformer language models. *arXiv preprint arXiv:2205.01068*, 2022.

## A. Other Related Works

The memory-augmented long-context transformer has been an active research topic in recent years. LongMem (Wang et al., 2024) chunks the long-document input into segments and caches the attention keys and values for each segment. During the inference of a segment, LongMem will select relevant key-value embedding pairs by computing the attention score between token embeddings and the cached key embeddings and fuse the top  $k$  embeddings. Memorizing Transformer (Wu et al., 2022) also caches the key-value embedding pairs similar to LongMem, but utilizes a kNN search to retrieve information similar to Unlimiformer. RET-LLM (Modarressi et al., 2023) employs prompt engineering to store the informative context in a database and search keywords when the context involves questions. While these works can precisely retrieve contexts, they are not scalable due to the **increasing memory consumption** of storing long contexts without compression. Segment-level recurrent models, such as EMMA (Moro et al., 2023), Memformer (Wu et al., 2020), and Transformer-XL (Dai et al., 2019), attempt to compress memory throughout the recurrence to reduce memory consumption. EMMA composes long-term memory from multiple short-term memory by linear combination and concatenates long and short-term memory to augment the segments. Transformer-XL propagates the compressed memory states derived from the attention of current layers to the previous layers for every iteration. Memformer augments the attention with the stored memory embeddings per time step and retrieves information using the cross-attention layer of the encoder-decoder model. However, Memformer employs a forgetting network to remove irrelevant context similar to LSTM, which can potentially delete useful contexts for unseen inputs. On the other hand, HMT compresses contexts into embeddings and retrieves information precisely without requiring a forgetting network to remove information permanently. Another issue with some of these works, including Memorizing Transformer, Memformer, Transformer-XL, and Unlimiformer, is that they need to fundamentally change the model architecture or inject new adapters based on different base model architecture. It makes deployment and extension to future LLMs very expensive. HMT avoids this issue by having a model-independent plug-and-play framework.

## B. Comparison to Unlimiformer

There are two major differences between a previous retrieval-augmented model, Unlimiformer (Bertsch et al., 2023), and HMT in terms of the memory recall mechanism:

- Unlimiformer retrieves the information with kNN search over the collection of encoded token segments, while HMT uses cross-attention. We believe there are several advantages of using cross-attention: (1) Attending Top K's most similar token segments still introduces information loss. Regarding the self-attention layer, the aggregation of tokens with less similar encodings may positively contribute to the quality of the final output. On the other hand, cross-attention fuses all cached hidden embeddings, weighted by the relative similarity, which captures the whole context. (2) The output of the cross-attention is a single embedding, which has lower computational overhead compared to attending  $k$  extra tokens.
- Each cached memory embedding encodes the current token segment and the previous memory embedding in HMT. Therefore, HMT can capture the whole context even with a limited number of cached embeddings. Memory recall is mainly used to rescale the importance of past information. On the other hand, the Unlimiformer needs to store all encodings, which is memory-consuming.

In terms of usage, Unlimiformer targets encoder-decoder models and injects retrieval modules into the backbone model. Although the authors recently added support for decoder-only models for token generation, only the Llama model architectures (Touvron et al., 2023) can be applied and the training/evaluation procedure is not specified. This is one of the biggest challenges for Unlimiformer to adapt to future LLMs for validation and generation. On the contrary, HMT focuses on decoder-only models. Since HMT does not inject new modules in the backbone model, it is effortless to adapt to future LLMs.

## C. Ablation Study of HMT Memory Recall Behavior

One insight of using memory recall in HMT is handling frequent context switching to previously discussed topics or new topics. To evaluate this property, we employ PubMedQA and artifact the dataset with multiple contexts, mentioned in Section 6.1. In this section, we will discuss other dataset manipulations on PG-19 to investigate the memory recall behavior of HMT further.

One way to manually introduce context switching is by interleaving the samples. For every 2 samples in the PG-19 dataset, we alternatively concatenate a segment of 256 tokens in each sample together to create a new sample. Therefore, a context switch will be invoked every 256 tokens. We fine-tuned and benchmarked HMT with Llama 2 7B over the artifact dataset. As a result, HMT can enhance the effectiveness of the baseline Llama 2 model, while RMT will worsen it, as shown in Figure 13. We record the context distance of memory recall for 30k-token input, illustrated in Figure 14, and notice a periodical recall distribution, indicating that HMT can capture the context-switching pattern.



Figure 13. Effectiveness of HMT and RMT with Llama 2 7B evaluated over PG-19 with interleaving sample. HMT is 12.02% better than RMT in terms of PPL for 2k to 100k-token samples.

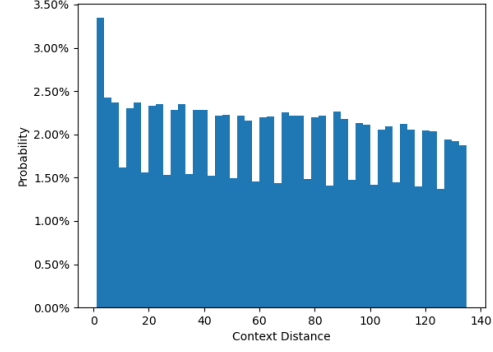


Figure 14. Histogram of context distance between the current segment and the segment corresponding to the memory embedding with the highest softmax score in the memory recall mechanism. The dataset evaluated is the PG-19 with interleaving samples.

To demonstrate that HMT’s behavior is aligned with the context-switching pattern, we further manipulate the PG-19 dataset by inserting 256 “\$” tokens for every 256 tokens to dilate each sample. Intuitively, the segment containing “\$” should be considered as irrelevant information and recalled infrequently. Figure 15 shows the memory recall pattern of HMT with Llama 2 7B over the diluted PG-19 dataset. We observe that HMT not only exhibits a periodical recall pattern but also successfully captures the position of irrelevant segments and avoids recalling them.

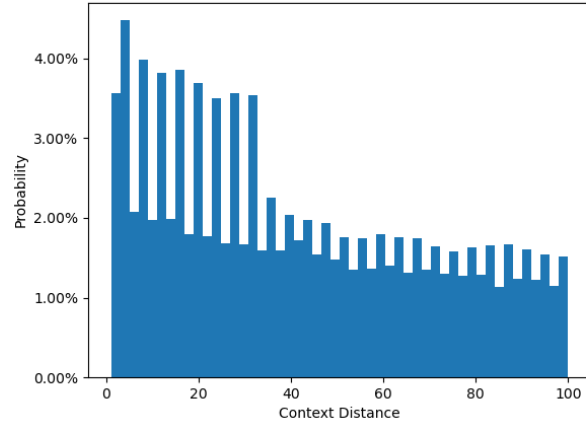


Figure 15. Histogram of context distance between the current segment and the segment corresponding to the memory embedding with the highest softmax score in the memory recall mechanism. The dataset evaluated is the diluted PG-19 dataset. Each sample is 25.6k tokens.

## D. Relationships Between Effectiveness and Size of Sensory Memory

During the experiment, we observed a general trend in the relationships between the effectiveness of HMT-augmented models and the size of sensory memory: the effectiveness will be first enhanced and then degraded as more and more embeddings are preserved for sensory memory. For instance, Table 6 illustrates the change of effectiveness of HMT + Llama 2 7B evaluated on Wikitext-103 with different sensory memory sizes. The PPL drops to the minimum when having 32 embeddings for the sensory memory.

Table 6. Effectiveness of HMT + Llama 2 7B evaluated on Wikitext-103 with 100k-token samples, with a various sensory memory size. The segment size is 256 tokens. The effectiveness improves and then degrades with an increasing number of embeddings that are preserved for sensory memory.

# OF EMBEDDINGS FOR SENSORY MEMORY	TEST PPL (WIKITEXT)
8	4.54
16	4.25
32	4.19
64	4.31
128	4.57

## E. Dataset Split for PubMedQA

The original PubMedQA dataset does not have training, validation, and test dataset splits. In the experiments, we choose the `pqa_artificial` subset and partition the training, validation, and test split, where the training split is the first 75% of samples, the validation split is the next 15% of samples, and the test split is the remaining 10% samples.

## F. Hardware Acceleration Consideration

The design of HMT can be implemented efficiently with customizable hardware, such as *Field-Programmable Gate Array* (FPGA). In contrast to GPUs, FPGA has two advantages in constructing accelerator HMT with high speed and low energy consumption:

**FPGA has a flexible architecture.** Users can define the FPGA fabric to have data-driven modules for stream architecture. Processing elements (PE) consume data from streams asynchronously and initiate computation once required data are ready. Stream architecture is naturally favored by the recurrent sequence models. Previous works in building an RNN accelerator (Chang & Culurciello, 2017; Khoda et al., 2023) and stream overlay for LSTM (Ioannou & Fahmy, 2022) on FPGA demonstrate a 1.25x to 16x throughput advantage over GPUs for low-batch tasks. Furthermore, the reconfigurable architecture allows fabric designers to save energy by only allocating necessary resources, instead of enforcing warp-level execution in GPUs (Abdelkhalik et al., 2022).

**FPGA has sophisticated support in task-level parallelism.** Frameworks such as TAPA (Guo et al., 2023) and PASTA (Khatti et al., 2023) generate multi-module FPGA designs with a single source file such that each function runs independently and communicates with FIFOs. On the contrary, the most popular GPU acceleration toolkit, CUDA, only has abstractions for task-level pipelining using stream (Li et al., 2014).

Based on the advantages of FPGA, we proposed the following optimizations for HMT:

**Intramodel Pipelining for Batched Inputs.** The transformer-based backbone model is naturally layered by multiple transformer blocks and the computation of each layer only depends on the previous layer. Therefore, the stream of inputs can be processed in the pipeline. Moreover, since the HMT processes long inputs in segments, the computation can further be pipelined with batches of inputs by round-robin scheduling.

**Task-Level Parallelism.** Although recalling memory requires the memory token from the inference of the previous segment, overlapping both tasks with an extra low-cost cross-attention computation is possible. When the model performs a forward pass on the current segment, the representation extraction of the next segment can generate the embedding  $H_n^{sum}$  and initiate the cross-attention with previous memory tokens for segments except the current one. The model will then wait until the memory token  $H_n^{mem}$  of the current segment is produced and compute the attention score between  $H_{n+1}^{sum}$  and  $H_n^{mem}$ .

Finally, the attention scores will be used to calculate the output embedding as the memory token for the next segment. Specifically, let  $H_{[n-N+1, n)}^{mem}$  be the embedding of memory tokens except for the current segment,  $H_n^{mem}$  be the memory token embedding of the current segment, and  $H_{n+1}^{sum}$  be the summary embedding of the next segment, the computation

$$K = H_{[n-N+1, n)}^{mem} W_k, Q = H_{n+1}^{sum} W_q, A = QK^T$$

can be overlapped with the forward pass of the previous segment and the computation

$$K_n = H_n^{mem} W_k, A_n = QK_n^T$$

$$H_n^S = \text{Softmax}\left(\frac{[A \circ A_n]}{\sqrt{d_h}}\right) [H_{[n-N+1, n)}^{mem} \circ H_n^{mem}]$$

will run in serial. Table 7 illustrates the runtime breakdown of each computation phase, proving that the latency of representation abstraction and computing cross-attention without the last memory token can be fully covered by the forward pass of the previous segment.

We leave the actual hardware implementation on an FPGA to future work.

Table 7. GPU Runtime breakdown of each step in memory recall mechanism of HMT per segment of inputs. The segment length is 256 and the backbone model is OPT 2.7B.

STEP	RUNTIME (MS)
FORWARD PASS OF THE SEGMENT	85.18
REPRESENTATION EXTRACTION	49.20
COMPUTE $A$	1.38
COMPUTE $A_n$	0.25

## G. Gradient Stability in HMT and RMT

In this section, we will formulate a mathematical description for the gradient stability of HMT when training with BPTT. BPTT with RMT behaves similarly to RNN which suffers from a vanishing or exploding gradient when there is a long chain of the gradient graph after unrolling (Pascanu et al., 2013). Specifically, for a generic RNN model with the following form:

$$H_t = \sigma(\mathbf{A}H_{t-1} + \mathbf{B}x_t)$$

where  $H_t$  is the hidden state at time  $t$ ,  $x_t$  is the input at time  $t$ , and  $\mathbf{A}$  and  $\mathbf{B}$  are parameters, the gradient will explode if  $\|\mathbf{A}^T\| > 1$  and vice versa. A similar phenomenon occurs when training segment-level recurrent models such as RMT. Here we provide a scratch calculation on the gradient of loss with respect to the memory token at the starting time, which is one of the parameters in both RMT and HMT, after  $t$  steps for RMT. Let  $y'_{t+1} = H(x_t, m_t)$  be the logits and  $m_{t+1} = F(x_t, m_t)$  be the generated memory embedding at time  $t$ , where  $x_t$  is the input,  $m_t$  is the memory token. The loss of inference is

$$L_{t+1} = \mathcal{L}(y'_{t+1}, y_{t+1}) \quad (1)$$

Therefore, the gradient can be calculated by the chain rule as

$$\begin{aligned} \frac{\partial L_{t+1}}{\partial m_0} &= \frac{\partial L_{t+1}}{\partial y'_{t+1}} \times \frac{\partial y'_{t+1}}{\partial m_0} \\ &= \frac{\partial L_{t+1}}{\partial y'_{t+1}} \times \frac{\partial H}{\partial m_t}(x_t) \times \frac{\partial m_t}{\partial m_0} \\ &= \frac{\partial L_{t+1}}{\partial y'_{t+1}} \times \frac{\partial H}{\partial m_t}(x_t) \times \prod_{i=0}^{t-1} \frac{\partial F}{\partial m_i}(x_i) \end{aligned} \quad (2)$$

Whether the gradient will explode or vanish depends on the input distribution and the function  $F_t$ . If  $\forall x_t, \frac{\partial F}{\partial m_t}(x_t) > 0$ , then the gradient will explode. Otherwise if  $\forall x_t, \frac{\partial F}{\partial m_t}(x_t) < 0$ , the gradient vanishes. Consequently, training RMT with

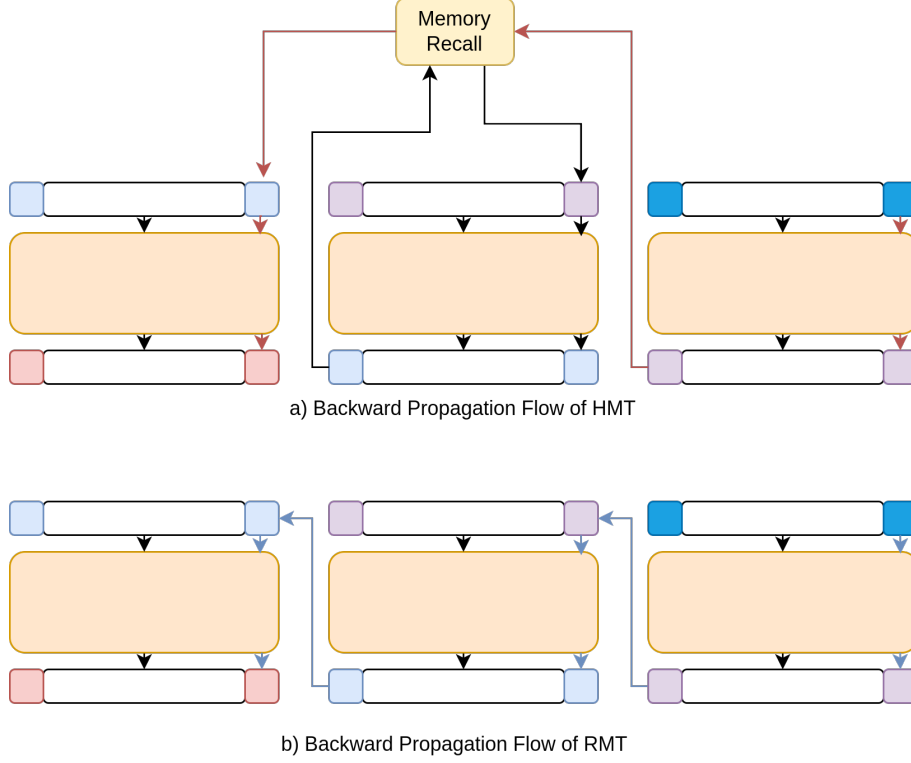


Figure 16. Backward propagation flows of HMT and RMT. The gradient of the first memorization prompt embedding (the red block on the right of the first segment) has multiple branches through the memory recall unit. On the contrary, the gradient for RMT requires propagating through each segment.

a very high BPTT unroll depth can be inefficient. For HMT, with the assistance of the memory recall mechanism, the gradient is not prone to explosion or vanishing. Intuitively, the backward propagation of HMT for the memorization prompt embedding contains multiple short sub-branches to prevent gradient vanishing and the memory recall mechanism can modulate the propagation chain to avoid gradient explosion, depicted in Figure 16. Let  $G_t(z_t, m_t, m_{t-1}, \dots, m_1) = m'_t$  be the memory search function where  $z_t$  is the representation extraction of segment at time  $t$ . Let  $s$  be the summarization token for representation extraction. The gradient for HMT is

$$\begin{aligned}
 \frac{\partial L_{t+1}}{\partial m_0} &= \frac{\partial L_{t+1}}{\partial y'_{t+1}} \times \frac{\partial y'_{t+1}}{\partial m_0} \\
 &= \frac{\partial L_{t+1}}{\partial y'_{t+1}} \times \frac{\partial H}{\partial m'_t}(x_t) \times \frac{\partial G_t}{\partial m_0} \\
 &= \frac{\partial L_{t+1}}{\partial y'_{t+1}} \times \frac{\partial H}{\partial m'_t}(x_t) \times \left( \sum_{k=1}^t \frac{\partial G_t}{\partial m_k}(z_k, m_t, \dots, m_{k-1}, m_{k+1}, \dots, m_1) \times \frac{\partial F}{\partial m_0} \right) \\
 &= \frac{\partial L_{t+1}}{\partial y'_{t+1}} \times \frac{\partial H}{\partial m'_t}(x_t) \times \left( \sum_{k=1}^t \frac{\partial G_t}{\partial m_k}(z_k, m_t, \dots, m_{k-1}, m_{k+1}, \dots, m_1) \times \frac{\partial F}{\partial m'_k} \times \frac{\partial G_{t-1}}{\partial m_0} \right) \\
 &= \dots
 \end{aligned} \tag{3}$$

The root cause of the gradient explosion or vanishing comes from the long chain of gradient products in the formulation. For HMT, there are multiple short branches of the multiplication chain after expanding the expression. The longest chain over all components in the gradient is

$$\frac{\partial L_{t+1}}{\partial y'_{t+1}} \times \frac{\partial H}{\partial m'_t}(x_t) \times \left( \prod_{k=1}^{t-1} \frac{\partial F}{\partial m'_k} \times \frac{\partial G_k}{\partial m_k} \right) \times \frac{\partial F}{\partial m_0} \tag{4}$$

For gradient vanishing, since  $\frac{\partial L_{t+1}}{\partial m_0}$  still has components with a shorter chain, the gradient will not disappear even when  $\left\| \frac{\partial F}{\partial m'_k} \times \frac{\partial G_k}{\partial m_k} \right\| < 1$ . For gradient explosion, empirically,  $\frac{\partial G_k}{\partial m_k}$  are different for each  $k$  by the property of cross attention and can modulate the term  $\frac{\partial F}{\partial m_k}$  to distribute near 1. Thus, HMT is less prone to gradient explosion.

A similar proof can be deduced for the segment-level summarization token embedding of HMT for representation extraction.

## H. Distributed Training with Memory Consumption Optimization

Although [Bulatov et al.](#) proves that unrolling more segments can improve the model effectiveness, they limit the number of segments unrolled to 4 with 2 NVIDIA A100 80GB GPUs since the maximum BPTT unroll depth is bounded by the GPU VRAM limit. There are three sources of VRAM consumption: model parameters, intermediate data (input segments, long-term memory, raw outputs of each segment, etc.), and optimization data (gradient and optimizer states). Although the computations of later segments do not require the intermediate data from the previous segment, the original BPTT will keep them on GPU by default. To reduce memory consumption, we customize the program to offload and load intermediate data for each input segment between the CPU and GPUs and distribute optimizer states and gradients throughout multiple GPUs running Zero Redundancy Optimizer (ZeRO) ([Rajbhandari et al., 2020](#)) Stage 2 in DeepSpeed ([Rasley et al., 2020](#)). These allow the model to unroll up to 15 segments with HMT. To train larger models, we employ LoRA ([Hu et al., 2021](#)) with rank 8. This allows us to fit 7B models to 4 MI210 GPUs.